Manuscript submitted to
AIMS' Journals
Volume **X**, Number **0X**, XX **200X**

Website: http://AIMsciences.org

pp. **X–XX**

Sue Ann Campbell

Department of Applied Mathematics
University of Waterloo
Waterloo ON N2L 3G1

Ilya Kobelevskiy

Imaging Research
Sunnybrook Health Sciences Centre
Toronto ON M4N 3M5 Canada

(Communicated by the associate editor name)

PHASE MODELS AND OSCILLATORS WITH TIME DELAYED COUPLING

Abstract. We consider two identical oscillators with time delayed coupling, modelled by a system of delay differential equations. We reduce the system of delay differential equations to a phase model where the time delay enters as a phase shift. By analyzing the phase model, we show how the time delay affects the stability of phase-locked periodic solutions and causes stability switching of in-phase and anti-phase solutions as the delay is increased. In particular, we show how the phase model can predict when the phase-flip bifurcation will occur in the original delay differential equation model. The results of the phase model analysis are applied to pairs of Morris-Lecar oscillators with diffusive or synaptic coupling and compared with numerical studies of the full system of delay differential equations.

1. **Introduction.** Coupled oscillators occur as models for many systems including neural networks [1, 2], laser arrays [3, 4], flashing of fireflies [5], cardiac pacemaker cells [6] and even movement of a slime mold [7]. A fundamental question about these systems is whether the elements will **phase-lock**, i.e., oscillate with some fixed phase difference, and how the strength of the coupling and other parameters in the model affect the answer to this question. In some systems, it is of particular interest whether the elements **synchronize**, i.e., phase-lock with zero phase difference. In many systems there are time delays in the connections between the oscillators due to the time for a signal to propagate from one element to the other. For example, in neural networks there is a delay due to conduction of electrical activity along an axon or a dendrite [8, 9]. This then adds the question of how the length of the time delay affects the phase-locking behaviour of the system.

The starting point of any study of coupled oscillators is usually to consider two reciprocally connected oscillators. One of the first observations in such models is that two fundamental phase-locked solutions may exist, the in-phase or synchronous solution (zero phase difference) and the anti-phase solution in which the two elements are one half period out of phase. Equivariant bifurcation theory has been used to study the existence of these two solutions for particular classes of oscillators [10, 11], however, proving stability is more difficult and is often model dependent.

2000 *Mathematics Subject Classification.* Primary: 58F15, 58F17; Secondary: 53C35.
Key words and phrases. Delay differential equations, phase models, coupled oscillators.

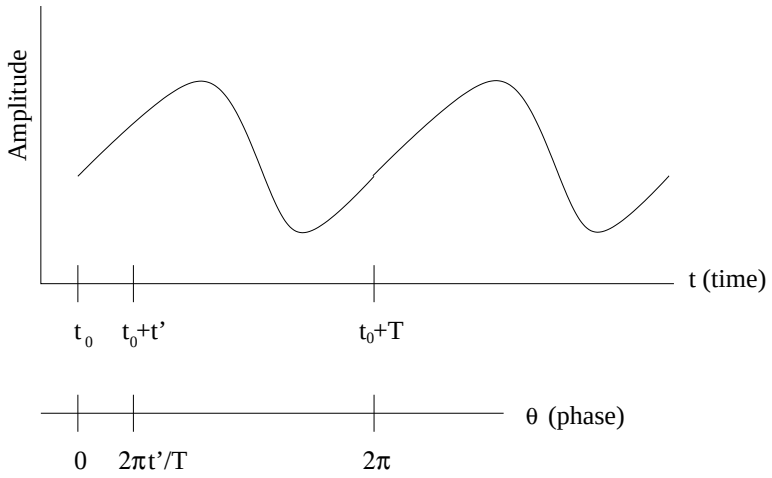

FIGURE 1. Defining the phase of an oscillator.

Below we review some of the literature on the stability of these two phase locked solutions, both as shown in models and observed in experiments.

Prasad et al. [12, 13] have done extensive studies of systems with delayed diffusive coupling:

$$\begin{aligned} \dot{\mathbf{x}}_1(t) &= \mathbf{F}_1(\mathbf{x}_1(t)) + \epsilon \mathbf{g}[\mathbf{x}_2(t-\tau), \mathbf{x}_1(t)] \\ \dot{\mathbf{x}}_2(t) &= \mathbf{F}_2(\mathbf{x}_2(t)) + \epsilon \mathbf{g}[\mathbf{x}_1(t-\tau), \mathbf{x}_2(t)], \end{aligned} \tag{1}$$

in the case that oscillators are identical, $\mathbf{F}_1 = \mathbf{F}_2$, or nearly identical. Using numerical simulations and analysis of Lypaunov exponents, they have characterized the **phase-flip** bifurcation: at a critical value of the delay the system switches from a stable in-phase state to a stable anti-phase state (or vice versa). This switch of stability is associated with a discrete change in the frequency of oscillation of the system. This bifurcation has also been documented in experimental systems [12, 14]. Transitions from in-phase to anti-phase oscillations have also been observed in human bimanual coordination experiments [15, 16, 17, 18], and in models of these experiments incorporating time delayed coupling [19].

Other studies show more complex transitions between in-phase and anti-phase solutions as the delay is varied. Intervals of values of τ where the two phase-locked states are **both** stable or regions where **neither** are stable, but other stable phase-locked solutions exist have also been found numerically and analytically using perturbation theory techniques [20, 21]. In slime mold experiments [7] regions of quasiperiodicity were observed between regions where the in-phase and anti-phase solutions are stable.

The references above primarily consider systems where the elements are inherently oscillatory, i.e., if the coupling is removed the elements still oscillate. Studies of systems where the elements are not inherently oscillatory (for example, excitable neural models) have also been done [22, 23, 24, 25, 26]. In these models it is often observed that there are regions where the system does not oscillate (i.e., regions of oscillator death) in between regions of stable in-phase and anti-phase solutions.

For systems with no time delay, phase models have been used to study phase locking, starting with the work of Kuramoto [27, 28]. A phase model represents each oscillator with a single variable as shown in Figure 1. For identical oscillators

and identical coupling the form of the model is

$$\begin{aligned} \frac{d\theta_1}{dt} &= \Omega + H(\theta_2 - \theta_1) \\ \frac{d\theta_2}{dt} &= \Omega + H(\theta_1 - \theta_2) \end{aligned}$$

where $\Omega = 2\pi/T$ is the angular frequency of the oscillators when uncoupled and H, the interaction function, represents the effect of the coupling. As we shall review in the next section, if the coupling is sufficiently weak, then a phase model representation of a system can be derived from a larger differential equation model. The literature on phase models falls into two types. Some studies focus on the analysis of general properties of phase models, given some assumptions on the interaction function, H, without linking the phase model to a particular differential equation model for the oscillator. For example see [5, 29, 30]. Other studies focus on deriving the phase model for a particular model or class of models and then determining the properties of the phase model. This latter approach has proved useful in studying synchronization properties of many different neural models [1, 8, 10, 31, 32, 33, 34]. Since the phase model can be linked to experimentally derived phase resetting curves [9], this approach has also been used to make predictions about synchronization properties of experimental preparations [33].

Initial studies of phase models for systems with delayed coupling considered models where the delay occurs in the argument of one of the phases [35, 36, 37, 38, 39]. For two oscillators this model is of the form:

$$\begin{aligned} \frac{d\theta_1}{dt} &= \Omega + H(\theta_1(t) - \theta_2(t-\tau)) \\ \frac{d\theta_2}{dt} &= \Omega + H(\theta_2(t) - \theta_1(t-\tau)) \end{aligned} \quad . \tag{2}$$

However, it has been shown [9, 40, 41] that for small enough time delays it is more appropriate to include the time delay as phase shift in the argument of the coupling function. Crook et al. [8] use this type of model to study a continuum of cortical oscillators with spatially decaying coupling and axonal delay. They show that for small delay the synchronous oscillation is stable, but for large enough delay the system undergoes a bifurcation where the synchronous oscillations lose stability and a travelling wave phase-locked solution becomes stable. Bressloff and Coombes [10, 42] study phase locking in chains and rings of pulse-coupled neurons with distributed delays and show that distributed delays result in phase models with a distribution of phase shifts. They consider phase models derived from integrate and fire neurons and the Kuramoto phase model, $H(\phi) = \sin(\phi)$. For the Kuramoto model in a ring configuration with excitatory coupling and several different types of delays, they show that the synchronous solution is stable for sufficiently small delay but loses stability as the delay is increased while a phase-locked travelling wave solution becomes stable. For the Kuramoto model with discrete delays they show that the stability of the synchronous solution periodically switches between stability and instability.

Following [9, 40, 41] the appropriate phase model for two oscillators with reciprocal time delayed coupling, with sufficiently small coupling and delay, is

$$\begin{aligned} \frac{d\theta_1}{dt} &= \Omega + H(\theta_1 - \theta_2 - \Omega\tau) \\ \frac{d\theta_2}{dt} &= \Omega + H(\theta_2 - \theta_1 - \Omega\tau) \end{aligned} .$$

Despite its simplicity, very little general work has been done on the effect of delay in this model. Thus, this is the focus of this paper. In the next section we briefly recall the steps involved in deriving this model and then obtain some results for a general interaction function, H. In the following section we consider some specific oscillators, derive the appropriate H function for them and apply the results of section 2. We then compare the phase model predictions with numerical studies of the corresponding delay differential equation model. Finally, in section 4 we discuss our results and draw conclusions.

2. Phase Model.

Consider the system of ODEs

$$\frac{d\mathbf{X}}{dt} = \mathbf{F}(\mathbf{X}(t)). \tag{3}$$

Assume that the system admits an exponentially asymptotically stable periodic orbit given by $\mathbf{X} = \hat{\mathbf{X}}(t),\ 0 \le t \le T = 2\pi/\Omega$. Linearizing (3) about the periodic orbit gives the periodic system

$$\frac{d\mathbf{X}}{dt} = D\mathbf{F}(\hat{\mathbf{X}}(t))\mathbf{X}.$$

The system adjoint to this is

$$\frac{d\mathbf{Z}}{dt} = -[D\mathbf{F}(\hat{\mathbf{X}}(t))]^T\mathbf{Z}. \tag{4}$$

Let $\mathbf{Z} = \hat{\mathbf{Z}}(t),\ 0 \le t \le T$ be the unique periodic solution of (4) satisfying the normalization condition

$$\frac{1}{T}\int_0^T \hat{\mathbf{Z}}(t)\cdot\mathbf{F}(\hat{\mathbf{X}}(t))\,dt = 1.$$

Next, consider a system of two identical coupled oscillators of the form (3):

$$\begin{aligned} \frac{d\mathbf{X}_1}{dt} &= \mathbf{F}(\mathbf{X}_1(t)) + \epsilon\mathbf{G}(\mathbf{X}_1(t), \mathbf{X}_2(t), \epsilon) \\ \frac{d\mathbf{X}_2}{dt} &= \mathbf{F}(\mathbf{X}_2(t)) + \epsilon\mathbf{G}(\mathbf{X}_2(t), \mathbf{X}_1(t), \epsilon) \end{aligned} \tag{5}$$

Assuming that ϵ is sufficiently small, one can apply weakly coupled oscillator theory [43, 44, 45, 46] to show that the phases of the oscillators of (5) satisfy

$$\begin{aligned} \frac{d\theta_1}{dt} &= \Omega + \epsilon H(\theta_2 - \theta_1) + O(\epsilon^2) \\ \frac{d\theta_2}{dt} &= \Omega + \epsilon H(\theta_1 - \theta_2) + O(\epsilon^2) \end{aligned} \tag{6}$$

where the interaction function, H, is given by

$$H(\theta_2 - \theta_1) = \frac{1}{T}\int_0^T \hat{\mathbf{Z}}(t)\mathbf{G}[\hat{\mathbf{X}}(t), \hat{\mathbf{X}}(t + (\theta_2 - \theta_1)/\Omega)]\,dt, \tag{7}$$

with $\hat{\mathbf{Z}}, \hat{\mathbf{X}}$ as defined above. Note that H is a $2\pi-$periodic function of its argument.

Now consider system (5) with time delayed coupling:

$$\begin{array}{rcl} \dfrac{d\mathbf{X}_1}{dt} &=& \mathbf{F}(\mathbf{X}_1(t)) + \epsilon\mathbf{G}(\mathbf{X}_1(t), \mathbf{X}_2(t-\tau), \epsilon) \\ \dfrac{d\mathbf{X}_2}{dt} &=& \mathbf{F}(\mathbf{X}_2(t)) + \epsilon\mathbf{G}(\mathbf{X}_2(t), \mathbf{X}_1(t-\tau), \epsilon) \end{array} . \tag{8}$$

This model includes the systems with delayed diffusive coupling, e.g., equation (1), as well as neural models with synaptic coupling and conduction delays.

Ermentrout [9, 40] has shown that the time delay enters as a phase shift in the coupling function. That is, using weakly coupled oscillator theory, the phases of the oscillators of (8) satisfy

$$\begin{array}{rcl} \dfrac{d\theta_1}{dt} &=& \Omega + \epsilon H(\theta_2 - \theta_1 - \Omega\tau) + O(\epsilon^2) \\ \dfrac{d\theta_2}{dt} &=& \Omega + \epsilon H(\theta_1 - \theta_2 - \Omega\tau) + O(\epsilon^2) \end{array} . \tag{9}$$

Izhikevich [41] refined this analysis, to show that (9) holds so long as $\Omega\tau = O(1)$ with respect to the small parameter ϵ, but if $\Omega\tau$ is large enough, i.e., $\Omega\tau = O(1/\epsilon)$ then (2) is the appropriate model. Introducing the phase difference $\phi = \theta_2 - \theta_1$ and dropping the terms that are higher order in ϵ, we obtain the phase model we will study:

$$\frac{d\phi}{dt} = -2\epsilon[H(\phi - \Omega\tau) - H(-\phi - \Omega\tau)] \stackrel{\text{def}}{=} -2\epsilon H_\tau(\phi). \tag{10}$$

Now the equilibrium points of (10) are given by ϕ^* such that $H_\tau(\phi^*) = 0$. Note that H_τ is a 2π periodic and odd function of ϕ, thus we need only consider the equilibrium points in $[0, 2\pi)$. Further, the following computation shows that H_τ is a $T-$periodic function of τ:

$$\begin{array}{rcl} H_{\tau+T}(\phi) &=& H(\phi - \Omega(\tau + T)) - H(-\phi - \Omega(\tau + T)) \\ &=& H(\phi - \Omega\tau - 2\pi) - H(-\phi - \Omega\tau - 2\pi) \\ &=& H_\tau(\phi). \end{array}$$

This leads to the following.

Proposition 1 (Existence of Equilibrium Points)**.**
For any interaction function H and any values of Ω and τ, the phase model (10) has the equilibrium points $\phi^* = 0$ and $\phi^* = \pi$. If $0 < \phi^* < \pi$ is an equilibrium point of (10) then so is $2\pi - \phi^*$, i.e., equilibrium points come in pairs, with one in $(0, \pi)$ and one in $(\pi, 2\pi)$. If ϕ^* is an equilibrium point of (10) at delay τ, then it is an equilibrium point at delays $\tau + kT$, $k \in \mathbb{Z}$.

Proof. Since H_τ is an odd, $2\pi-$periodic function of ϕ, it follows that

$$H_\tau(0) = -H_\tau(0) \Rightarrow H_\tau(0) = 0$$

and

$$H_\tau(\pi) = H_\tau(\pi - 2\pi) = H_\tau(-\pi) = -H_\tau(\pi) \Rightarrow H_\tau(\pi) = 0.$$

Thus 0 and π are equilibrium points of (10).

Further, if ϕ^* is equilibrium point of (10) then

$$H_\tau(\phi^*) = 0 \Rightarrow H_\tau(2\pi - \phi^*) = H_\tau(-\phi^*) = 0.$$

Thus $2\pi - \phi^*$ is an equilibrium point of (10).

The last result follows from the periodicity of H_τ with respect to τ. □

Since $\phi^* = 0$ corresponds to the synchronous or in-phase phase-locked solution of the original model (8), we will refer to it as the **in-phase equilibrium point**. Similarly, we will refer to $\phi^* = \pi$ as the **anti-phase equilibrium point**.

Let us now consider the stability of an equilibrium point ϕ^* of (10). The linear (local) stability of ϕ^* is determined by the sign of $H'_\tau(\phi^*)$. If $H'_\tau(\phi^*) > 0$ then the equilibrium point is asymptotically stable and if $H'_\tau(\phi^*) < 0$ it is unstable. If $H'_\tau(\phi^*) = 0$, the stability is not determined by the linearization. Now

$$H'_\tau(\phi) = H'(\phi - \Omega\tau) + H'(-\phi - \Omega\tau), \tag{11}$$

thus the stability of the equilibrium points will, in general, depend on H, Ω and τ. In particular, there are simple formulas that determine the stability of the in-phase and anti-phase equilibrium points:

$$H'_\tau(0) = 2H'(-\Omega\tau) \quad \text{and} \quad H'_\tau(\pi) = 2H'(\pi - \Omega\tau). \tag{12}$$

We can now establish the following.

Proposition 2 (Stability of Equilibrium Points)**.**
For any interaction function H we have the following.

1. *The equilibrium points ϕ^* and $2\pi - \phi^*$ have the same stability.*
2. *The stability of the in-phase equilibrium point at delay τ is the same as that of the anti-phase equilibrium point at delay $\tau + T/2$.*
3. *If an equilibrium point ϕ^* undergoes a delay induced change of stability at $\tau = \tau_c$, then it will have a countable number of stability switches in $\tau > 0$.*
4. *The in-phase and anti-phase equilibrium points have a countable number of stability switches in $\tau > 0$.*

Proof. The first result follows from the fact that $H'_\tau(\phi)$, as defined by (11), is a $2\pi-$periodic function of ϕ.

The second result follows from the following computation

$$\begin{aligned} H'_{\tau+T/2}(\pi) &= H'(\pi - \Omega(\tau + T/2)) + H'(-\pi - \Omega(\tau + T/2)) \\ &= H'(\pi - \Omega\tau - \pi) + H'(-\pi - \Omega\tau - \pi) \\ &= 2H'(-\Omega\tau) \\ &= H'_\tau(0). \end{aligned}$$

Since H'_τ is a $T-$periodic function of τ, if the stability of an equilibrium point ϕ^* changes, say, from stable to unstable, at some value $\tau = \tau_c$ then it will have the same change of stability at $\tau = \tau_c + kT$, $k = 1, 2, \ldots$. Since H'_τ is a continuous function of τ it follows that the equilibrium point must change stability from unstable to stable at least once in each interval $(\tau_c + (k-1)T, \tau_c + kT)$. The third result follows.

Since $H(\phi)$ is a $2\pi-$periodic function it must have at least one maximum and one minimum in $[0, 2\pi)$. Let $\phi_{\max}$ and $\phi_{\min}$ be the values of ϕ where these occur. Then $H'(\phi_{\max}) = 0 = H'(\phi_{\min})$ and consideration of the sign of $H'(\phi)$ near $\phi_{\max}$ and $\phi_{\min}$ shows that the stability of the in-phase equilibrium point changes from stable to unstable at $\tau = T(1 - \phi_{\min}/(2\pi))$ and from unstable to stable at $\tau = T(1 - \phi_{\max}/(2\pi))$. Result 3 then implies that the in-phase equilibrium point has a countable number of stability switches in $\tau > 0$. Result 2 then gives the result for the anti-phase equilibrium point. □

It follows from the proof above that the in-phase equilibrium points will switch from stable to unstable when

$$\tau = T(k + 1 - \frac{\phi_{\min}}{2\pi}),\ k = 0, 1, \ldots$$

and from unstable to stable when

$$\tau = T(k + 1 - \frac{\phi_{\max}}{2\pi}),\ k = 0, 1, \ldots$$

where $\phi_{\min}$ and $\phi_{\max}$ are values where $H(\phi)$ has a minimum and maximum, respectively. Similarly, the anti-phase equilibrium points will switch from stable to unstable when

$$\tau = T(k + 1/2 - \frac{\phi_{\min}}{2\pi}),\ k = 0, 1, \ldots$$

and from unstable to stable when

$$\tau = T(k + 1/2 - \frac{\phi_{\max}}{2\pi}),\ k = 0, 1, \ldots$$

Thus there will be intervals of τ where the in-phase equilibrium point is stable interleaved with intervals where the anti-phase equilibrium point is stable. The exact nature of the interleaving will depend on the relationship between $\phi_{\min}, \phi_{\max}$ and T, however, we can determine conditions for a phase-flip bifurcation to occur. Since this bifurcation corresponds to the simultaneous changing of the stability of the in-phase and anti-phase equilibrium points, a simple calculation shows that it will occur if

$$\phi_{\max} - \phi_{min} = \pm\pi.$$

In applying phase model reduction above to a particular model one can usually only calculate the interaction function H, i.e., evaluate eq. (7), numerically. Thus, to study the system with delayed coupling, one needs a way to represent H_τ. One way to do this is using the Fourier modes of H which can easily be computed from the numerical representation of H. Writing H in terms of its Fourier series expansion

$$H(\phi) = a_0 + \sum_{n=1}^{\infty} [a_n \cos(n\phi) + b_n \sin(n\phi)], \tag{13}$$

H_τ can be expressed as

$$H_\tau(\phi) = \sum_{n=1}^{\infty} c_n(\tau) \sin(n\phi), \tag{14}$$

where

$$\begin{aligned} c_n(\tau) &= b_n \cos(n\Omega\tau) + a_n \sin(n\Omega\tau) \\ &= r_n \sin(n\Omega\tau - \delta_n) \end{aligned} \tag{15}$$

with

$$r_n = \sqrt{a_n^2 + b_n^2} \quad \text{and} \quad \delta_n = \arctan\left(\frac{-b_n}{a_n}\right).$$

Note that when $\tau = 0$ we have

$$H_\tau(\phi) = \sum_{n=1}^{\infty} b_n \sin(n\phi),$$

i.e., H_τ is the odd part of H, as expected [45]. However, for $\tau > 0$ H_τ depends on both the odd and even parts of H.

The Fourier approach is useful since we can usually approximate H, and hence H_τ, by a finite number of Fourier modes. Thus we can get approximate analytic expression for the phase model:

$$\frac{d\phi}{dt} = -2\epsilon \sum_{n=1}^{N} c_n(\tau)\sin(n\phi) \tag{16}$$

which may be amenable to analysis if the number of modes in the approximation, N, is not too large.

In many papers, H is assumed to be represented by the first set of Fourier modes. The following proposition gives some exact results in this case.

Proposition 3. *If the interaction function H can be represented by the first set of Fourier modes, i.e.,*

$$H(\phi) = a_0 + a_1\cos(\phi) + b_1\sin(\phi) \tag{17}$$

then we have the following

1. *The only equilibrium points of (10) are the in-phase and anti-phase ones, i.e., $\phi^* = 0, \pi$.*
2. *These equilibrium points have opposite stability, i.e., when the in-phase equilibrium point is asymptotically stable then the anti-phase one is unstable and vice versa.*
3. *As τ is increased, these equilibrium points will switch stability periodically at the values*

$$\tau = T\left[\frac{1}{2\pi}\arctan\left(\frac{-b_1}{a_1}\right) + \frac{k}{2}\right], \quad k = 0, 1, 2, \ldots. \tag{18}$$

4. *At the switching points, the frequencies of the corresponding in-phase and anti-phase phase-locked oscillations will differ by the amount $2\sqrt{a_1^2 + b_1^2}$.*

Proof. If H satisfies (17), then the phase model (10) becomes

$$\frac{d\phi}{dt} = -2\epsilon c_1(\tau)\sin(\phi) = -2\epsilon H_\tau(\phi) \tag{19}$$

Clearly $H_\tau(\phi)$ has only two zeros in $[0, 2\pi)$: $\phi = 0$ and $\phi = \pi$ which gives the first result. Further, $H'_\tau(0) = c_1(\tau) = -H'_\tau(\pi)$ which gives the second result. Setting $c_1(\tau)$ equal to zero and solving for τ gives the third result.

Now from equation (9), on a phase-locked solution with phase difference ϕ^* the frequencies of the two oscillators will be

$$\Omega_* = \Omega + H(\phi^* - \Omega\tau). \tag{20}$$

Evaluating this for $\phi^* = 0$ and π at the bifurcation points defined by (18) gives

$$\Omega_0 = \Omega + a_0 \mp \sqrt{a_1^2 + b_1^2}, \quad \Omega_\pi = \Omega + a_0 \pm \sqrt{a_1^2 + b_1^2}.$$

The fourth result follows. □

The previous proposition proves that the phase-flip bifurcation occurs in system (8), if the coupling is sufficiently weak and the interaction function satisfies (17), and gives a formula for the frequency jump at the bifurcation. This bifurcation is degenerate since two equilibrium points change stability simultaneously. The degeneracy is easily seen in the phase model (19) since at the bifurcation point $H_\tau \equiv 0$. One should not expect to see such a bifurcation generically. Equivalently, for a generic oscillator, it should not be expected that the Fourier expansion of H

would only have the first modes. (For example, in the model of [8] they use five modes to get a good representation of H.) However, if the coefficients of the higher Fourier modes are small enough that H is close to (17) then one might still expect to see something similar to a phase-flip bifurcation where the change of stability of the in-phase and anti-phase solutions occur close together but not at the same value of the delay. We will see examples of this in the next section.

3. **Example: Morris-Lecar oscillators.** In this section we take the ideas of the previous section and apply them to a particular example: a system of two Morris-Lecar oscillators with time delayed coupling. The Morris-Lecar model was introduced to study the oscillations in barnacle muscle fibre [47]. It is a useful model since it is two dimensional and exhibits excitability and oscillations with variables that can be directly linked to physiological variables.

We use the dimensionless formulation of the Morris-Lecar model due to Rinzel and Ermentrout [48]:

$$\begin{aligned} v' &= -g_{Ca} m_\infty(v)(v-1) - g_K\, w\,(v-v_K) - g_L\,(v-v_L) + i \\ &\stackrel{def}{=} f(v,w) \\ w' &= \phi\,\lambda(v)\,(w - w_\infty(v)) \end{aligned} \tag{21}$$

where

$$\begin{aligned} m_\infty(v) &= \frac{1}{2}\,(1+\tanh((v-\nu_1)/\nu_2)) \\ w_\infty(v) &= \frac{1}{2}\,(1+\tanh((v-\nu_3)/\nu_4)) \\ \lambda(v) &= \cosh((v-\nu_3)/(2\nu_4)) \end{aligned}$$

Detailed studies of this system have been made showing it can exhibit a variety of behaviour [49]. In our study we consider two sets of parameter values, given in Table 1, for which the system has a unique, exponentially asymptotically stable limit cycle. The limit cycles are created by different bifurcations as we now describe. For the parameter values as in Table 1 and $g_{Ca} = 1$ the system has a stable limit

TABLE 1. Values of parameters used in the Morris-Lecar model.

Values of parameters which are the same for both parameter sets			
Parameter	Name	Value	
v_{Ca}	Calcium equilibrium potential	1	
v_K	Potassium equilibrium potential	-0.7	
v_L	Leak equilibrium potential	-0.5	
g_K	Potassium ionic conductance	2	
g_L	Leak ionic conductance	0.5	
ϕ	Potassium rate constant	$\frac{1}{3}$	
v_1	Calcium activation potential	-0.01	
v_2	Calcium reciprocal slope	0.15	
v_3	Potassium activation potential	0.1	
v_4	Potassium reciprocal slope	0.145	
Values of parameters that differ for set I and set II			
Parameter	Name	Set I value	Set II value
g_{Ca}	Calcium ionic conductance	1	0.5
i	Applied current	0.09	0.15

cycle that is created by a saddle node on an invariant circle (SNIC) bifurcation at

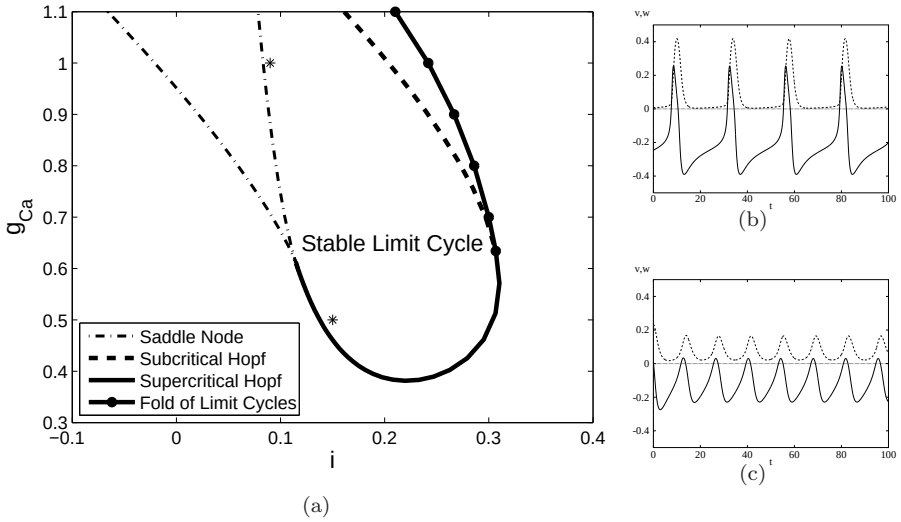

FIGURE 2. (a) Two parameter bifurcation diagram for the Morris-Lecar model (21). Stable limit cycles exist in the region bounded by the saddle node, supercritical Hopf and fold of limit cycles bifurcations. The parameter sets I and II as given in Table 1 are marked with *'s. (b) Limit cycle for parameter set I. (c) Limit cycle for parameter set II. Solid line corresponds to v, dashed to w.

$i \approx 0.08326$ and lost in a fold of limit cycles at $i \approx 0.2419$. See Figure 2(a). For $g_{Ca} = 1$, $i = 0.09$, the system has a unique stable limit cycle with period $T \approx 23.87$, as shown in Figure 2(b). For the parameter values as in Table 1 and $g_{Ca} = 0.5$, the system has a stable limit cycle it is created in a supercritical Hopf bifurcation at $i \approx 0.1377$ and lost in another supercritical Hopf bifurcation at $i \approx 0.3044$. See Figure 2(a). For $g_{Ca} = 0.5$ and $i = 0.15$ the system has a unique stable limit cycle with period $T = 13.81$, as shown in Figure 2(c). Note that the limit cycle corresponding to parameter set I has a relaxation oscillator shape, where as the oscillation corresponding to parameter set II is more sinusoidal in shape.

3.1. **Diffusive Coupling.** Now consider two identical Morris-Lecar oscillators with time delayed diffusive coupling of the form considered in [12, 13, 22, 23, 50]. This leads to the following system of delay differential equations:

$$\begin{aligned} v_1'(t) &= f(v_1(t), w_1(t)) + \epsilon(v_2(t-\tau) - v_1(t)) \\ w_1'(t) &= \phi\,\lambda(v_1(t))\,(w_1(t) - w_\infty(v_1(t))) \\ v_2'(t) &= f(v_2(t), w_2(t)) + \epsilon(v_1(t-\tau) - v_2(t)) \\ w_2'(t) &= \phi\,\lambda(v_2(t))\,(w_2(t) - w_\infty(v_2(t))) \end{aligned} \tag{22}$$

We used the software XPPAUT [51] to calculate the interaction functions, H, for this model with $\tau = 0$ and to find the first 10 terms in the Fourier series approximation for H. Figure 3 shows the interaction functions, H, together with the approximations using one and four Fourier modes. Clearly one mode is not enough to capture the full shape of H, however, the approximation with four modes is

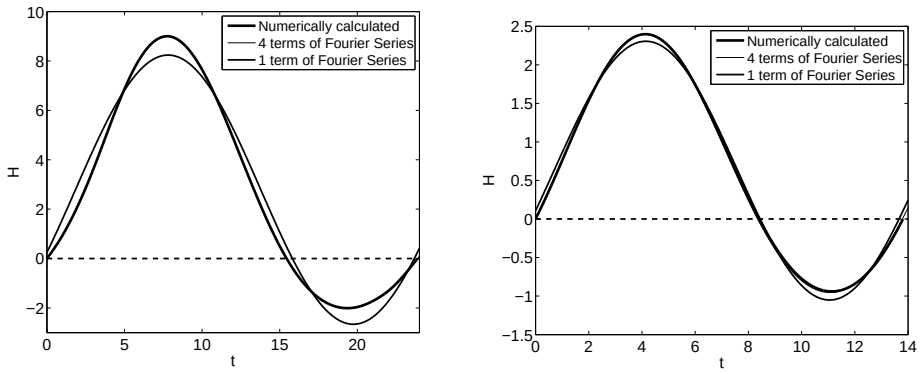

(a) Parameter Set I (b) Parameter Set II

FIGURE 3. Interaction functions for Morris-Lecar model (22) with parameter sets as given in Table 1, together with the approximations using 1 and 4 terms of Fourier Series.

TABLE 2. Fourier coefficients of the interaction function for the Morris-Lecar model (22).

	Parameter set I		Parameter set II	
j	a_j	b_j	a_j	b_j
0	2.915252	0	0.6271561	0
1	-2.684797	4.908449	-0.5209326	1.595618
2	-0.3278022	-0.7020183	-0.08538575	-0.04727176
3	0.05596774	-0.09934668	-0.005648281	-0.00301241
4	0.0351635	-0.01104474	-0.0002642404	-0.002760313

indistinguishable. This can be explained by consideration of the Fourier coefficients in Table 2.

Now, using the results discussed in the previous section, we can make some predictions about the behaviour of the phase model for this system. Recall that any zero, ϕ^*, of H_τ corresponds to an equilibrium point of the phase model and that this solution will be asymptotically stable (unstable) if $H'_\tau(\phi^*) > 0$ (< 0). To begin, consider the in-phase and anti-phase equilibrium points, i.e., $\phi^* = 0$ and π, which are guaranteed to exist. From equation (12) and Figure 3 it is clear that for both parameter sets the in-phase equilibrium point will be stable at $\tau = 0$ while the anti-phase equilibrium point will be unstable. Further, by estimating the maximum and minimum points of H from Figure 3 one could use the formulas given after Proposition 2 to predict where the changes of stability for these equilibrium points occur. More accurate information is obtained by studying the zeros of H_τ numerically. We have done this in XPPAUT [51], using the first four terms of the Fourier series for H. The results are shown in Figure 4. We find that behaviour is quite similar to that predicted by Proposition 3: the equilibrium points switch stability periodically in τ and the stability of the in-phase and anti-phase equilibrium points are almost always the opposite of each other. Using the values for the period

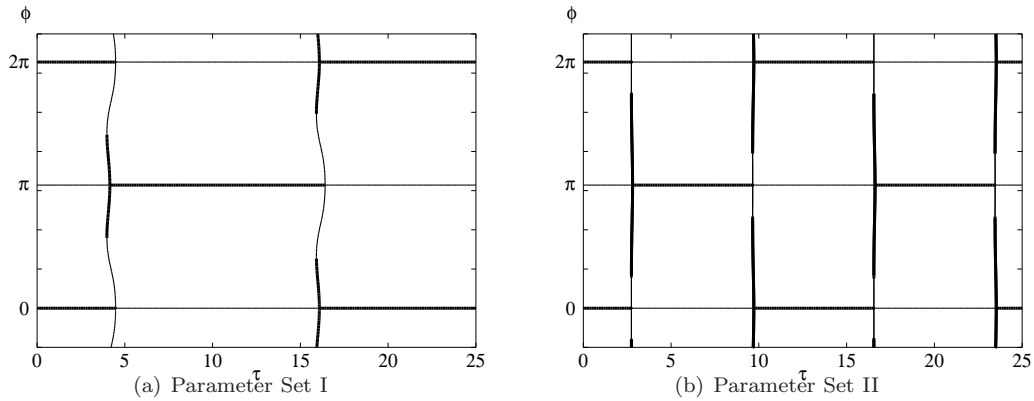

(a) Parameter Set I (b) Parameter Set II

FIGURE 4. Numerical bifurcation diagram with respect to τ for the phase model (16) with $N = 4$ corresponding to the Morris-Lecar model (22). Thick/thin lines correspond to stable/unstable equilibrium points. The period is $T \approx 23.87$ for parameter set I and $T \approx 13.81$ for parameter set II.

and the Fourier coefficients, we can evaluate the switching points given by (18):

$$\begin{array}{lrcl} \text{Parameter set I:} & \tau & \approx & 4.07 + 11.94k, \\ \text{Parameter set II:} & \tau & \approx & 2.76 + 6.91k, \end{array} \qquad k = 0, 1, \ldots$$

which are close to the values seen in Figure 4.

Closer examination of Figure 4 shows that the stabilities of the in-phase and anti-phase equilibrium points do not switch at exactly the same value of τ. For parameter set I, there are small intervals of τ where both equilibrium points are stable and, for parameter set II, there are small intervals where they are both unstable. To clarify the behaviour near these points, we show the bifurcation diagrams zoomed close to one switching point in Figure 5. In both cases, we see that the transition from stable in-phase equilibrium point to stable anti-phase equilibrium point involves two pitchfork bifurcations and one saddle node bifurcation. The difference between the two cases occurs due to the relative ordering of the pitchfork bifurcations. For parameter set I the pitchfork bifurcation stabilizing the anti-phase equilibrium point occurs before the pitchfork bifurcation destabilizing the in-phase equilibrium point. For parameter set II the ordering is the opposite. As expected from the analysis of the previous section, the identical sequence, with the roles of the in-phase and anti-phase equilibrium points reversed, occurs for τ one half period later and the whole bifurcation structure repeats periodically in τ with period T. We note that we must include enough terms in the Fourier series to resolve the bifurcation structure. For both parameter sets, if fewer than three modes are used then the present bifurcation diagram changes drastically. For three or more modes, the structure is the same, the additional modes only slightly modify the bifurcation points.

3.1.1. *Comparison with the full model.* We performed numerical simulations on the full system of delay differential equations (22) using the package XPPAUT. The parameter values used are as given in Table 1, with various values of τ and ϵ. The initial conditions used were of the form

$$(v_1(t), w_1(t), v_2(t), w_2(t)) = (v_{10}, w_{10}, v_{20}, w_{20}) \quad -\tau \le t \le 0. \tag{23}$$

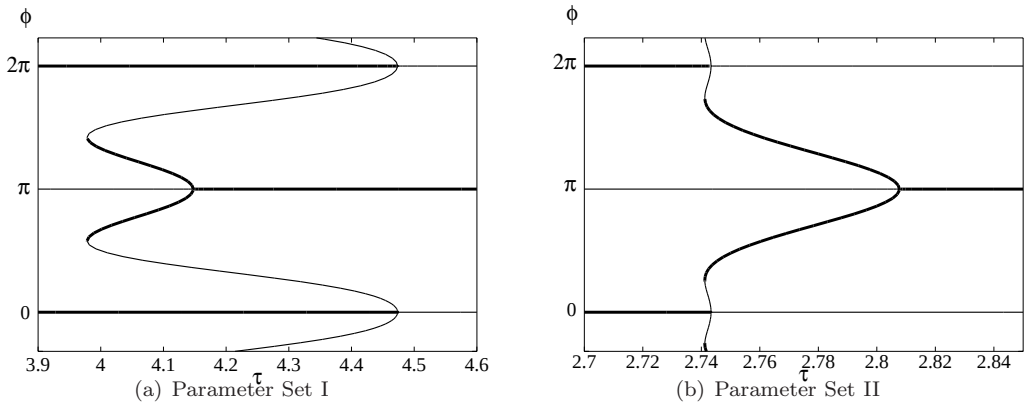

(a) Parameter Set I (b) Parameter Set II

FIGURE 5. Close up of the numerical bifurcation diagrams of Figure 4. Thick/thin lines correspond to stable/unstable equilibrium points.

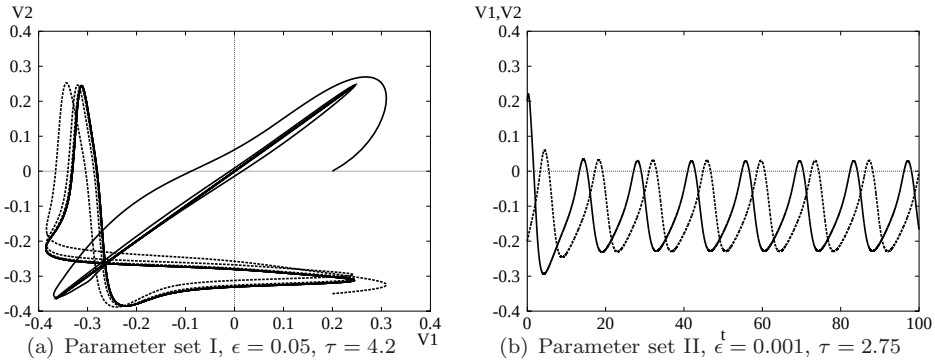

(a) Parameter set I, $\epsilon = 0.05$, $\tau = 4.2$ (b) Parameter set II, $\epsilon = 0.001$, $\tau = 2.75$

FIGURE 6. Numerical simulations of the full Morris-Lecar model (22). (a) Coexistence of in-phase and anti-phase periodic solutions. Initial conditions were of the form (23) with $(v_{10}, w_{10}, v_{20}, w_{20}) = (0.2, 0.01, 0, 0.01)$ and $(0.2, 0.01, -0.35, -0.01)$. (b) Phase locked solution. Initial condition was of the form (23) with $(v_{10}, w_{10}, v_{20}, w_{20}) = (0.2, 0.01, -0.2, -0.01)$. See Table 1 for parameter values.

Some example simulations are shown in Figure 6. For parameter set I with $\tau = 4.2$ and $\epsilon = 0.05$ we observed the coexistence of stable in-phase and anti-phase periodic solutions. For parameter set II with $\tau = 2.75$ and $\epsilon = 0.001$, we observed the existence of a stable phase-locked solution which is neither in-phase nor anti-phase. These simulations agree with the prediction of the phase model, as shown in Figure 5.

To make a more comprehensive comparison between the predictions of the phase model and the behaviour of the full model (22) we use the numerical continuation software DDE-BIFTOOL [52]. Using this software, we were able to follow the in-phase and anti-phase period solutions of (22) and calculate their stability as τ is increased. The results for several values of ϵ are shown in Figure 7. The switching

TABLE 3. Values of τ where changes of stability occur. Four Fourier modes are used in the phase model.

Solution	Phase Model	Full Model	
		$\epsilon = 0.001$	$\epsilon = 0.01$
Parameter Set I			
In-phase	4.47	4.64	4.89
	16.08	15.94	14.75
	28.36	28.54	29.21
	39.97	39.59	36.40
Anti-phase	4.15	4.09	3.84
	16.41	16.59	17.06
	28.02	27.74	25.67
	40.28	40.54	41.60
Parameter Set II			
In-phase	2.74	2.85	2.94
	9.71	9.55	9.39
	16.55	16.65	16.84
	23.52	23.35	22.89
	30.36	30.45	30.79
	37.33	37.15	36.25
	44.18	44.35	44.75
Anti-phase	2.81	2.65	2.65
	9.64	9.75	9.85
	16.62	16.45	16.15
	23.45	23.55	23.85
	30.43	30.25	29.65
	37.26	37.45	37.75
	44.25	44.05	43.15

points for both parameter sets are summarized in Table 3. For $\epsilon = 0.001$ the agreement with the predictions of the phase model is excellent, but as ϵ is increased the agreement becomes less good. By $\epsilon = 0.1$ it is clear that the phase model is no longer appropriate. For this value of ϵ we see significant variation in the amplitude of the limit cycle with τ and coexistence of multiple, stable in-phase and anti-phase periodic solutions.

3.2. **Synaptic coupling.** We now consider the same model as above but with the diffusive coupling replaced by synaptic coupling:

$$\begin{aligned} v_1'(t) &= f(v_1(t), w_1(t)) + \epsilon s(v_2(t-\tau))(v_1(t) - E_{\text{syn}}) \\ w_1'(t) &= \phi\, \lambda(v_1(t))\, (w_1(t) - w_\infty(v_1(t))) \\ v_2'(t) &= f(v_2(t), w_2(t)) + \epsilon s(v_1(t-\tau))(v_2(t) - E_{\text{syn}}) \\ w_2'(t) &= \phi\, \lambda(v_2(t))\, (w_2(t) - w_\infty(v_2(t))) \end{aligned} \tag{24}$$

where

$$s(v) = 0.5\,(1 + \tanh(10v))$$

and ϵ is the maximal synaptic strength. This model falls into our general framework (8), thus the predictions of section 2 should apply for ϵ sufficiently small.

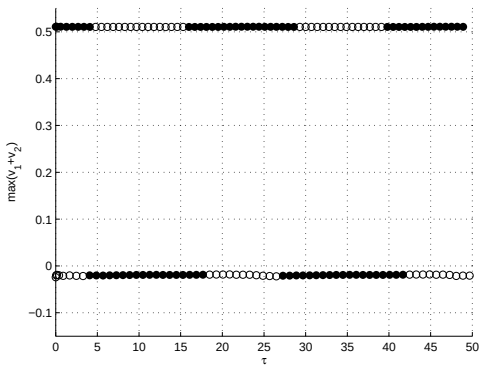

(a) Parameter set I, $\epsilon = 0.001$

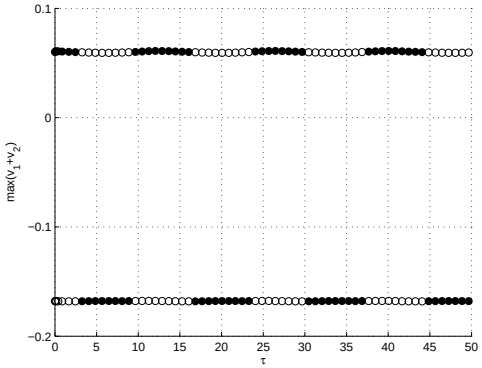

(b) Parameter set II, $\epsilon = 0.001$

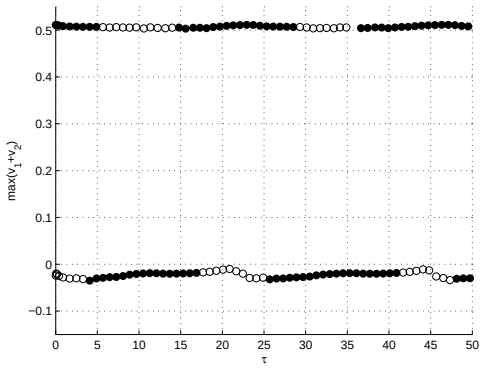

(c) Parameter set I, $\epsilon = 0.01$

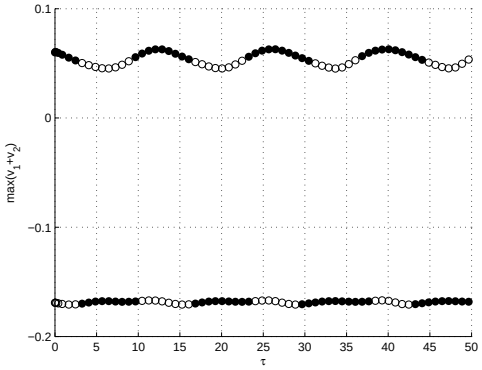

(d) Parameter set II, $\epsilon = 0.01$

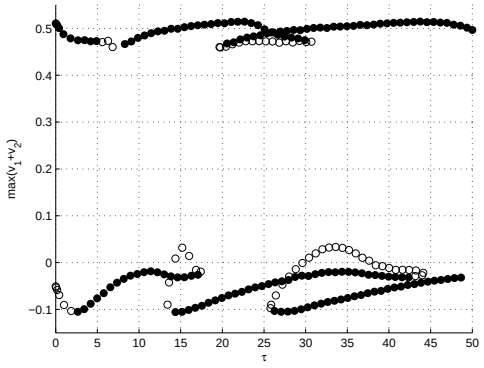

(e) Parameter set I, $\epsilon = 0.1$

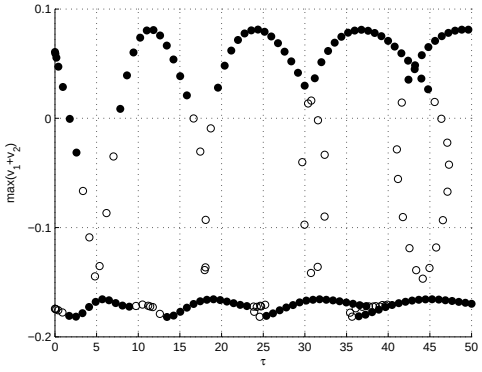

(f) Parameter set II, $\epsilon = 0.1$

FIGURE 7. Results from numerical continuation study of in-phase and anti-phase periodic solutions in the Morris-Lecar model (22) with parameter values as given in Table 1 and ϵ as shown. The amplitude of the periodic solutions (represented as $\max(v_1(t) + v_2(t))$, $0 \le t \le T$) is plotted vs the time delay, τ. In all cases, the upper curve corresponds to the in-phase solution and the lower curve and the anti-phase solution. Filled/open circles denote stable/unstable solutions.

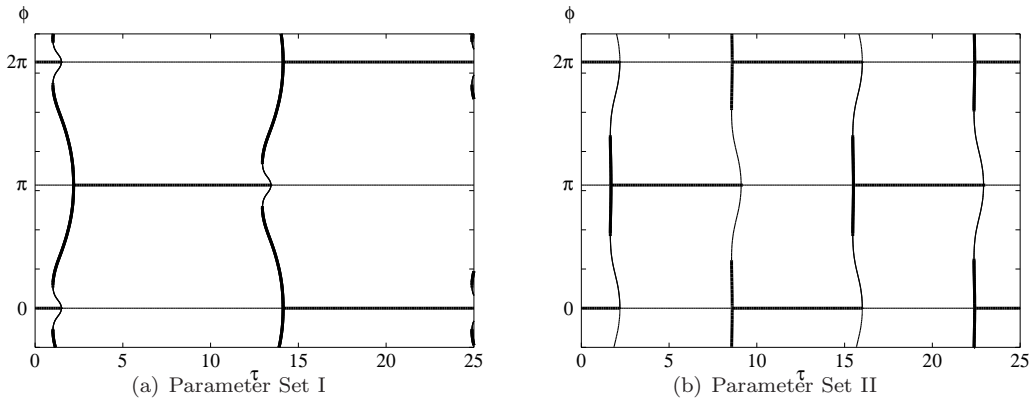

(a) Parameter Set I (b) Parameter Set II

FIGURE 8. Numerical bifurcation diagram with respect to τ for the phase model (16) corresponding to the Morris-Lecar model (24). Thick/thin lines correspond to stable/unstable equilibrium points. Four terms of the Fourier series for H are used for parameter set I, seven for parameter set II. The period is $T \approx 23.87$ for parameter set I and $T \approx 13.81$ for parameter set II.

Computing the interaction function and its Fourier series as before, we found bifurcation diagrams for the (approximate) phase model (16) as shown in Figure 8. The bifurcation sequence here is similar to that observed with diffusive coupling, with some slight differences. In particular, the ordering of the bifurcations is changed. In this case parameter set I has intervals of τ where neither in-phase nor anti-phase solutions are stable, while for parameter set II there are intervals where both are stable. Also, changes of stability for the in-phase and anti-phase solutions are further apart and the initial instability (where the in-phase oscillation loses stability) occurs for a smaller value of τ. For comparison, numerical continuation studies of the full delay differential equation model (24) are shown in Figure 9. Once again, the phase model represents the full system well for ϵ sufficiently small, but loses validity for larger ϵ. The phase model seems to be a better match for $\epsilon = 0.01$ with synaptic coupling than with diffusive coupling.

4. **Conclusions.** In this paper we studied a phase model for two coupled identical oscillators with delayed connections. For any interaction function, H, we showed that as the delay is increased, a countable number of stability switches of the in-phase and anti-phase solutions must occur. These stability switches occur periodically in τ with period equal to the intrinsic period of the uncoupled oscillator. We proved that the phase-flip bifurcation, i.e., the in-phase and anti-phase oscillations switch stability at the same value of τ, occurs if the coupling is sufficiently weak and the interaction function is simple, i.e., $H(\phi) \approx a_0 + a_1 \cos(\phi) + b_1 \sin(\phi)$. We also gave a formula for the frequency jump at the phase-flip bifurcation in terms of the coefficients a_1 and b_1. We conjectured that for an oscillator with H close to this ideal form, i.e., the coefficients of the higher Fourier modes are small, then a "near phase-flip" bifurcation would occur where the change of stability of the in-phase and anti-phase solutions occur close together but not at exactly the same value of the delay.

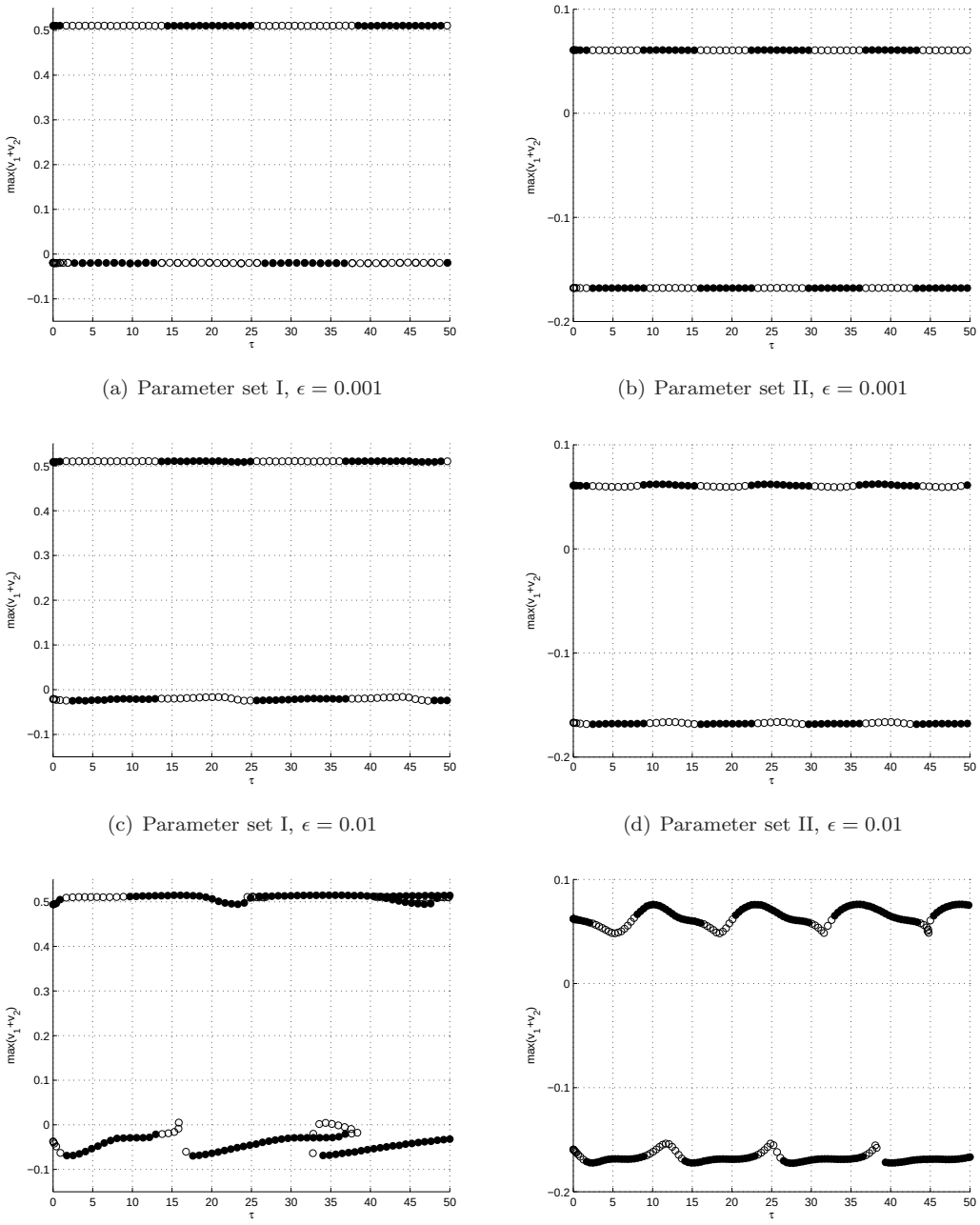

(a) Parameter set I, $\epsilon = 0.001$

(b) Parameter set II, $\epsilon = 0.001$

(c) Parameter set I, $\epsilon = 0.01$

(d) Parameter set II, $\epsilon = 0.01$

(e) Parameter set I, $\epsilon = 0.1$

(f) Parameter set II, $\epsilon = 0.1$

FIGURE 9. Results from numerical continuation study of in-phase and anti-phase periodic solutions in the Morris-Lecar model (24) with parameter values as given in Table 1 and ϵ as shown. The amplitude of the periodic solutions (represented as $\max(v_1(t) + v_2(t))$, $0 \le t \le T$) is plotted vs the time delay, τ. In all cases, the upper curve corresponds to the in-phase solution and the lower curve and the anti-phase solution. Filled/open circles denote stable/unstable periodic orbits.

As an example we considered a pair of Morris-Lecar oscillators with delayed diffusive or synaptic coupling. We considered two sets of parameter values. For the first set, the uncoupled system was close to a SNIC bifurcation and the resulting oscillations were high amplitude with a relaxation oscillator shape. For the second set, the uncoupled system was close to a super-critical Hopf bifurcation and thus the oscillations were lower amplitude and more sinusoidal in shape.

For the model with diffusive coupling we did see "near" phase-flip bifurcations and showed that between the switches of stability of the in-phase and anti-phase solutions there are a number of secondary bifurcations involving phase-locked oscillations with phase shifts between 0 and π. The exact sequence of bifurcations depended on the particular oscillators present, but involved both pitchfork bifurcations and saddle node bifurcations. For the model with synaptic coupling, the switches of stability of the in-phase and anti-phase solutions occurred further apart, although the sequence of bifurcations between them was similar to that seen with diffusive coupling. Numerical continuation studies of the full delay differential equation models verified that predictions of the phase model were valid for sufficiently small coupling.

The results should also apply to other oscillators. To test this, we considered the Van der Pol-Fitzhugh-Nagumo with diffusive coupling studied by Prasad et al. [12]. In numerical studies of this model, Prasad et al. [12] observe a phase-flip bifurcation, where the in-phase solution loses stability and the anti-phase gains stability, at a particular value of the delay. At this point they observe the angular frequency jumps from ~ 3.5 to ~ 4. (See [12, Fig. 3]). We calculated the appropriate phase model interaction function for the model of Prasad et al. and found that it was reasonably well fit by the first few Fourier modes. Thus the phase model predicts that the switches of stability of the in-phase and anti-phase solutions should be close to a phase-flip bifurcation. The phase model predicts a jump of 0.4455 in the angular frequency at this bifurcation. These results agree qualitatively with the numerical studies of Prasad et al. We verified that quantitative agreement between the phase model and the full delay differential equation model is obtained if smaller coupling values are used than those in the study of Prasad et al.

We can also make a prediction about the robustness of synchronization to delays. Consider a pair of identical coupled oscillators which are synchronized, i.e. the in-phase solution is stable, when there is no delay in the coupling. We showed that the in-phase solution will lose stability when

$$\tau = T\left(1 - \frac{\phi_{\min}}{2\pi}\right)$$

where T is the intrinsic period of the uncoupled oscillators, and $\phi_{\min}$ is the phase where there is a minimum in the interaction function for the phase model of the system with no delay. Thus longer periods will tend to make oscillators more robust to delays. We did observe this in the Morris-Lecar model with diffusive coupling: the in-phase solution remained stable for larger delay in the parameter set corresponding to the longer period.

While the phase model is expected only to be valid for sufficiently small coupling, in our examples, we observed that the qualitative behaviour, e.g., the switching of stabilities of the in-phase and anti-phase solutions, persisted for reasonably large coupling. This is not surprising given the continuous dependence of models on the coupling strength.

There are many ways that the work of this paper could be generalized. An obvious first step is to consider larger networks. The results of Bressloff and Coombes [10, Section 4.4] for the Kuramoto model in a ring configuration indicate that generalization of our Proposition 3 to that configuration should be possible. For networks with identical neurons and all-to-all coupling, many more solution types are possible, such as clustered solutions and the splay-phase state [29]. It would be interesting to consider the effect of time delay on these solutions.

Acknowledgements. This work has benefitted from the support of the Natural Sciences and Engineering Research Council of Canada. We would like to thank the reviewers for their suggestions which greatly improved the presentation of this paper.

REFERENCES

[1] D. Hansel, G. Mato, and C. Meunier, *Phase dynamics for weakly coupled Hodgkin-Huxley neurons*, Europhys. Lett., **23** (1993), 367–372.

[2] N. Kopell and G.B. Ermentrout, *Coupled oscillators and the design of central pattern generators*, Math. Biosci., **90** (1988), 87–109.

[3] H.G. Winful and S.S. Wang, *Dynamics of phaselocked semiconductor laser arrays*, Appl. Phys. Lett., **52** (1988), 1774 –1776.

[4] H.G. Winful and S.S. Wang, *Stability of phase locking in coupled semiconductor laser arrays*, Applied Physics Letters, **53** (1988), 1894–1896.

[5] R.E. Mirollo and S.H. Strogatz, *Synchronization of pulse-coupled biological oscillators*, SIAM J. Appl. Math., **50** (1990), 1645–1662.

[6] C.S. Peskin, "Mathematical aspects of heart physiology", Courant Institute of Mathematical Sciences, New York University, New York, NY, 1975.

[7] A. Takamatsu, T. Fujii, and I. Endo, *Time delay effect in a living coupled oscillator system with plasmodium of* physarum polycephalum, Phys. Rev. E, **85** (2000), 2026–2029.

[8] S.M. Crook, G.B. Ermentrout, M.C. Vanier, and J.M. Bower, *The role of axonal delay in synchronization of networks of coupled cortical oscillators*, J. Comp. Neurosci., **4** (1997), 161–172.

[9] N. Kopell and G.B. Ermentrout, *Mechanisms of phase-locking and frequency control in pairs of coupled neural oscillators*, in "Handbook of dynamical systems, vol 2: Toward applications" (eds. B Fiedler), Elsevier, 2002.

[10] P. Bressloff and S. Coombes, *Symmetry and phase-locking in a ring of pulse-coupled oscillators with distributed delays*, Physica D, **126** (1999), 99–122.

[11] P. Kitanov, "Normal form analysis for bifurcations with Huygens symmetry", PhD thesis, University of Guelph, Canada, 2011.

[12] A. Prasad, S. Kumar Dana, R. Karnatak, J. Kurths, B. Blasius, and R. Ramaswamy, *Universal occurence of the phase-flip bifurcation in time-delay coupled systems*, CHAOS, **18** (2008), 023111.

[13] A. Prasad, J. Kurths, S. Kumar Dana, and R. Ramaswamy, *Phase-flip bifurcation induced by time delay*, Phys. Rev. E, **74** (2006), 035204.

[14] J. M. Cruz, J. Escalona, P. Parmananda, R. Karnatak, A. Prasad, and R. Ramaswamy, *Phase-flip transition in coupled electrochemical cells*, Phys. Rev. E, **81** (2010), 046213.

[15] R.G. Carson, W.D. Byblow, and D. Goodman, *The dynamical substructure of bimanual coordination*, in "Interlimb coordination: Neural, dynamical and cognitive constraints" (eds. S Swinnen, H Heuer, J Massion, and P Casaer), Academic Press, 1994, 319–337.

[16] K.J. Jantzen and J.A.S. Kelso, *Neural coordination dynamics of human sensorimotor behaviour: A review*, in "Handbook of brain connectivity" (eds. R McIntosh and VK Jirsa), Springer-Verlag, 2007.

[17] J.A.S. Kelso, *Phase transitions and critical behaviour in human bimanual coordination*, Am. J. Physiol. - Reg. I, **15** (1984), R1000–R1004.

[18] J.A.S. Kelso, K.G. Holt, P. Rubin, and P.N. Kugler, *Patterns of human interlimb coordination emerge from nonlinear limit cycle oscillatory processes: theory and data*, J. Motor Behav., **13** (1981), 226–261.

[19] H. Haken, J.A.S. Kelso, and H. Bunz, *A theoretical model of phase transitions in human hand movements*, Biol. Cybern., **51** (1985), 347–356.
[20] A.K. Sen and R. Rand, *A numerical investigation of the dynamics of a system of two time-delayed coupled relaxation oscillators*, Comm. Pur. Appl. Math., **2** (2003), 567–577.
[21] S. Wirkus and R. Rand, *The dynamics of two coupled van der Pol oscillators with delay coupling*, Nonlinear Dynam., **30** (2002), 205–221.
[22] N. Burić and D. Todorović, *Dynamics of Fitzhugh-Nagumo excitable systems with delayed coupling*, Phys. Rev. E, **67** (2003), 066222.
[23] N. Burić and D. Todorović, *Bifurcations due to small time-lag in coupled excitable systems*, Int. J. Bifurc. Chaos, **15** (2005), 1775–1785.
[24] S.A. Campbell, R. Edwards, and P. van den Dreissche, *Delayed coupling between two neural network loops*, SIAM J. Appl. Math., **65** (2004), 316–335.
[25] M.A. Dahlem, G. Hiller, A. Panchuk, and E. Schöll, *Dynamics of delay-coupled excitable neural systems*, Int. J. Bifurc. Chaos, **29** (2009), 745–753.
[26] E. Schöll, G. Hiller, P. Hövel, and M. A. Dahlem, *Time-delay feedback in neurosystems*, Philos. T. R. Soc. A, **367** (2009), 1079–10956.
[27] Y. Kuramoto, *Cooperative dynamics of oscillator community. A study based on lattice of rings.*, Prog. Theor. Phys. Suppl., (1984), 223–240.
[28] Y. Kuramoto and I Nishikawa, *Statistical macrodynamics of large dynamical systems. Case of phase transition in oscillator communities.*, J. Stat. Phys., **49** (1987), 569–605.
[29] K. Okuda, *Variety and generality of clustering in globally coupled oscillators*, Physica D, **63** (1993), 424–436.
[30] Y.-X. Li, Y.-Q. Wang, and R. Miura, *Clustering in small networks of excitatory neurons with heterogeneous coupling strengths*, J. Comp. Neurosci., **14** (2003), 139–159.
[31] G.B. Ermentrout, *Type I membranes, phase resetting curves, and synchrony*, Neural Comput., **8** (1996), 979–1001.
[32] D. Hansel, G. Mato, and C. Meunier, *Synchrony in excitatory neural networks*, Neural Comput., **7** (1995), 307–337.
[33] J.G. Mancilla, T.J. Lewis, D.J. Pinto, J. Rinzel, and B.W. Connors, *Synchronization of electrically coupled pairs of inhibitory interneurons in neocortex*, J. Neurosci., **27** (2007), 2058–2073.
[34] T. Zahid and F.K. Skinner, *Predicting synchronous and asynchronous network groupings of hippocampal interneurons coupled with dendritic gap junctions.*, Brain Res., **1262** (2009), 115–129.
[35] S. Kim, S. H. Park, and C.S. Ryu, *Multistability in coupled oscillator systems with time delay*, Phys. Rev. Lett., **79** (1997), 2911–2914.
[36] T. Luzyanina, *Synchronization in an oscillator neural network model with time-delayed coupling*, Network: Comput. Neural Sys., **6** (1995), 43–59.
[37] E. Niebur, H.G. Schuster, and D.M. Kammen, *Collective frequencies and metastability in networks of limit-cycle oscillators with time delay*, Phys. Rev. Lett., **67** (1991), 2753–2756.
[38] H.G. Schuster and P. Wagner, *Mutual entrainment of two limit cycle oscillators with time delayed coupling*, Prog. Theor. Phys., **82** (1989).
[39] M.K.S. Yeung and S.H. Strogatz, *Time delay in the Kuramoto model of coupled oscillators*, Phys. Rev. Lett., **82** (1999), 648–651.
[40] G.B. Ermentrout, *An introduction to neural oscillators*, in "Neural modelling and neural networks" (eds. F. Ventriglia), Pergamon, 1994, 79–110.
[41] E.M. Izhikevich, *Phase models with explicit time delays*, Phys. Rev. E, **58** (1998), 905–908.
[42] P. Bressloff and S. Coombes, *Travelling waves in chains of pulse-coupled integrate-and-fire oscillators with distributed delays*, Physica D, **130** (1999), 232–254.
[43] G.B. Ermentrout and N. Kopell, *Frequency plateaus in a chain of weakly coupled oscillators, I*, SIAM J. Math. Anal., **15** (1984), 215–237.
[44] G.B. Ermentrout and N. Kopell, *Multiple pulse interactions and averaging in couple neural oscillators*, J. Math. Biol., **29** (1991), 195–217.
[45] G.B. Ermentrout and D.H. Terman, "Mathematical foundations of neuroscience", Springer, New York, NY, 2010.
[46] F.C. Hoppensteadt and E.M. Izhikevich, "Weakly connected neural networks", Springer-Verlag, New York, 1997.
[47] C. Morris and H. Lecar, *Voltage oscillations in the barnacle giant muscle fibre*, Biophys. J., **35** (1981), 193–213.

[48] J. Rinzel and G.B. Ermentrout, *Analysis of neural excitability and neural oscillations*, in "Methods in neuronal modeling: From synapses to networks" (eds. C. Koch and I. Segev), MIT Press, 1989.

[49] K. Tsumoto, H. Kitajima, T. Yoshinaga, K. Aihara, and H. Kawakami, *Bifurcations in the Morris-Lecar neuron model*, Neurocomputing, **69** (2006), 293–316.

[50] N. Burić, I. Grozdanović, and N. Vasović, *Type I vs type II excitable systems with delayed coupling*, Chaos Solitons Fract., **23** (2005), 1221–1233.

[51] G.B. Ermentrout, "Simulating, analyzing and animating dynamical systems: A guide to xppaut for researcher and students.", SIAM, Philadelphia, PA, 2002.

[52] K Engelborghs, T Luzyanina, and G Samaey, "DDE-BIFTOOL v. 2.00: a MATLAB package for bifurcation analysis of delay differential equations.", Technical Report TW-330, Department of Computer Science, K.U. Leuven, Leuven, Belgium, 2001.

E-mail address: sacampbell@uwaterloo.ca